DOI 10.1007/s10511-020-09626-3
Astrophysics, Vol. 63, No. 2, June, 2020

VARIATIONS IN THE PERIOD OF NEGATIVE SUPERHUMPS IN SU UMa-TYPE DWARF NOVAE. I. MN Dra (2012-2017)

A. S. Sklyanov,[1] E. P. Pavlenko,[2] K. A. Antonyuk,[2] N. V. Pit,[2] V. P. Malanushenko,[3] A. V. Shchurova,[4] A.-M. A. Zaostrozhnykh,[1] S. Yu. Shugarov,[4,5] A. A. Sosnovskij,[2] Ju. V. Babina,[2] O. I. Antonyuk,[2] A. O. Simon,[6] R. Ya. Zhuchkov,[1] and A. G. Gutaev[1]

This is a photometric study of the dwarf nova MN Dra made during 2012-2017 on nine telescopes over 152 nights. Overall, the observations covered 4 superoutbursts, 7 normal outbursts and the quiescent state. The interval between neighboring superoutbursts in 2017 was 65 days, and between neighboring normal bursts, 15 days. During he superoutbursts of 2012 and 2017, positive superhumps with a period of 0.10558(6) and 0.10500(2) days, respectively, were observed and in the quiescent state, negative superhumps with an average period of 0.095921(3) days, It is shown that the period of the negative superhumps varied cyclically between normal outbursts: sharply decreasing during an outburst and gradually increasing toward the onset of the next outburst. This feature of the variation in the period of the negative superhumps may correspond to a rapid increase in the radius of the accretion disk during the time of an outburst followed by a slow decrease, in agreement with the theory of thermal-tidal instability.

Keywords: *MN Dra: cataclysmic variables: negative superhumps: evolution of negative superhumps; accretion*

(1) Kazan Federal University, Kazan, Russia
(2) Crimean Astrophysical Observatory, Crimea; e-mail: eppavelenko@gmail.com
(3) Apache Point Observatory, University of New Mexico, USA
(4) Institute of Astronomy, Slovak Academy of Sciences, Slovakia
(5) P. K. Shternberg State Institute of Astronomy, M. V. Lomonosov Moscow State University, Moscow, Russia
(6) Taras Shevchenko Kiev National University, Kiev, Ukraine

Original article submitted August 25, 2019. Translated from Astrofizika, Vol. 63, No. 2, pp. 227-243 (May 2020)

1. Introduction

Cataclysmic variables are a type of close binary system consisting of a white dwarf (the main component) and an evolved Main sequence star (the secondary component) that fills its Roche cavity. Matter from the secondary component flows to the main component through an internal Lagrange point to form an accretion disk around the white dwarf [1].

Dwarf novae are a subtype of cataclysmic variable. These systems are characterized by the presence of regular outbursts with amplitudes of 2^m-6^m and typically last from a few days to several weeks. The mechanism for these outbursts is assumed to be the development of a thermal instability in the accretion disk [1].

SU UMa are a subclass of dwarf novae. Their distinctive feature is the existence of two types of outbursts: normal outbursts lasting a few days and superoutbursts lasting up to 2-3 weeks. The orbital periods of SU UMa-type stars range from 76 min to ~3.18 h [2].

Superoutbursts are ascribed to the development of a tidal instability in the accretion disk caused by the attainment by the outer radius of the disk of a 3:1 resonance between the rotations of the disk and the secondary component [3]. The characteristic time between successive superoutbursts is referred to as the supercycle of a given system. The tidal instability causes the accretion disk to become elliptical and the line of apsides undergoes precession. Apsidal precession leads to the appearance of oscillations in the star's brightness with a period several percent greater than the orbital period of the system. These oscillations, which can be observed during superoutbursts, are referred to as positive superhumps [3]. The periods of superhumps evolve during a superoutburst and can, in general, pass through 3 stages A, B, and C [4].

Besides positive superhumps, some cataclysmic variables have been found to have brightness oscillations with periods a few percent shorter than the orbital period. These oscillations are known as "negative superhumps" [5-7]. The are associated with the appearance of a nodal precession of the accretion disk owing to which a stream of overflowing material will collide with the accretion disk at different distances, depending on the inclination of the disk and it orientation relative to the secondary component [7-10]. At present there is no unique answer regarding the cause of the inclination of the accretion disk. The following have been proposed as possible mechanisms: an interaction between the disk and a stream of overflowing matter [11-13], tidal effects caused by the secondary component [14-17], radiation from the main component [17-24], the magnetic field of the secondary component [25], the magnetic field of the main component [18, 26, 27], etc. It has has been shown that for successful detection of brightness variation associated with nodal precession it is necessary that the inclination of the accretion disk be at least 4° [28]. In SU UMa-type dwarf novae, negative superhumps are usually observed only in the quiescent state and during normal outbursts. There are three objects which are an exception – ER UMa, V1504 Cyg, and V344 Lyr, for which they have been observed during superoutbursts [29-32].

The distribution of the orbital periods of cataclysmic variables has a considerably smaller number of systems with periods in the range of 2.15 to 3.18 h. This interval has come to be known as the "period gap" and is related to switching of the basic mechanism for loss of angular momentum by the system [2].

The star MN Dra was discovered by Antipin in archives of photographic plates in 2001. At first it was designated as Var73 Dra. In the subsequent campaign this system was classified as an SU UMa-type dwarf nova with an orbital period lying within the "period gap" [33]. The period of the positive superhumps was found to be $0^d.0954$, but a probable day-associated period of $0^d.104$ was not excluded. The interval between neighboring normal outbursts was relatively short, about 8 days [33]. Yet another campaign of observations of this star followed in 2002-2003 [34]. The period of the superhumps was refined to $0^d.104885(93)$. The supercycle of the system was determined to be ~60 days. A periodicity in the brightness minimum was also observed with a period of $0^d.10424(3)$ [34]. This served as a basis for the assumption that permanent positive superhumps are observed in this star. In 2009 the period of the brightness oscillations in the quiescent state was refined to 0.096 days, so it could be identified as the period of negative superhumps [35]. The orbital period of the system was estimated by Pavlenko, et al. [35], to be $0^d.0998(2)$ and Bakowska, et al., as $0^d.0994(1)$ [36]. Pavlenko, et al. [35], first revealed that the period of the negative superhumps has a tendency to increase on approaching a normal outburst. Further observations in that same year confirmed the presence of negative superhumps with a mean period of $0^d.095952$. The authors showed that a tendency toward an increase in the period of the negative superhumps toward the onset of a normal outburst was observed for at least two cycles [37]. We note that the interval between normal outbursts was then 15-16 days, or twice that in 2001. In 2014, Kato, et al. [38], first gave estimates of the mass ratio of the components in this system: $q=0.327$ and $q=0.258$. In 2018 the supercycle of this star was reported [36] to have increased to 74±0.5 days.

This paper is a detailed study of the evolution of the negative superhumps during time of the supercycle for several observational seasons.

2. Observations and data reduction

Several campaigns for observing the star MN Dra were conducted during 2012-2017 over 152 nights on nine telescopes without using color filters. Information on these observations is given in Table 1. The campaign in 2012 lasted from 3 June to 19 November on the AZT-11 (1.25-m, ProLine PL23042 CCD) telescope at the Crimean Astrophysical Observatory (CrAO), "Astrotel" (30-cm, Alta 9000 Apogee CCD) at Kazan Federal University, ARCSAT (50-cm, APOGEE U-47UV CCD) at the Apache Point Observatory (USA). These observations covered 82 nights. In 2013, this object was observed on one night at the ZTSh telescope. In 2017 the observations proceeded from 28 April to 25 November for 63 nights on the K-380 telescope (38-cm, APOGEE ALTA E47 array), AZT-11 (1.25-m, ProLine PL23042 array) and ZTSh (2.6-m, APOGEE ALTA E47 array) at CrAO, the SKAS telescope (28-cm, QSI 583wsg array) at Kazan Federal University, the AZT-8 telescope (70-cm, FLI PL4710 array) at the observation station of the Lesniki station of Kiev National University, the Zeiss 60 (60-cm, Fli-ML3041 array) and 18-cm telescope (18-cm, SBIG ST-10XME array) at the Stara Lesna observation station of the Slovak Academy of Sciences, and the Zeiss 60 (60-cm, Ap47p array), AZT-5 (50-cm, Apogee Alta U16M array), and ZTE (1.25-m, VersArray-1300 array) telescopes at the Nauchnyi station of the Crimean Astronomical Observatory of the GAISh of Moscow State University. The quality of the observing conditions defined in terms of the half width of the image of a star (FWHM) was better than 3".5 on most of the nights. The observational data were subjected to standard processing and calibration in

TABLE 1a. Observation Log

Telescope	Start-end of observations JD-2456000		Telescope	Start-end of observations JD-2456000		Telescope	Start-end of observations JD-2456000	
				2012				
ARCSAT	082.7316	082.8401	ARCSAT	109.7768	109.9504	AZT-11	178.2494	178.3979
ARCSAT	085.7210	085.8464	ARCSAT	110.7863	110.9442	AZT-11	182.2387	182.3690
ARCSAT	086.7039	086.8267	ARCSAT	111.7785	111.8303	AZT-11	183.2742	183.4234
AZT-11	087.3102	087.3940	AZT-11	119.4392	119.5305	AZT-11	185.2174	185.3243
ARCSAT	087.7101	087.8408	AZT-11	121.3490	121.4453	AZT-11	187.2219	187.3224
AZT-11	088.2977	088.3019	AZT-11	130.3571	130.5509	Astrotel	203.2172	203.5897
ARCSAT	088.7007	088.8477	AZT-11	131.3008	131.4682	Astrotel	207.3530	207.5909
AZT-11	089.2874	089.3920	Astrotel	133.2431	133.3064	Astrotel	208.3475	208.4648
ARCSAT	089.7107	089.8362	Astrotel	134.2402	134.5267	Astrotel	211.2989	211.4871
ARCSAT	090.6996	090.8251	Astrotel	135.2546	135.5381	Astrotel	214.2129	214.5197
AZT-11	091.3086	091.4468	Astrotel	136.2462	136.3042	ARCSAT	226.5878	226.8011
ARCSAT	091.8160	091.9415	Astrotel	138.2446	138.3107	ARCSAT	227.5816	227.7960
AZT-11	092.3840	092.5158	Astrotel	140.3192	140.5225	ARCSAT	228.5504	228.7897
ARCSAT	092.8231	092.9437	Astrotel	142.2417	142.5435	ARCSAT	230.6901	230.8065
ARCSAT	093.8176	093.9442	Astrotel	143.3146	143.5178	ARCSAT	231.6157	231.7939
AZT-11	094.3191	094.3966	Astrotel	148.2870	148.4000	ARCSAT	232.5906	232.7725
AZT-11	095.2971	095.3955	Astrotel	152.2330	152.2852	ARCSAT	233.5975	233.7693
AZT-11	098.3308	098.4626	Astrotel	157.2709	157.5404	ARCSAT	235.5581	235.7875
AZT-11	099.2821	099.4140	Astrotel	160.3418	160.5559	ARCSAT	236.5718	236.7689
ARCSAT	099.7865	099.9457	Astrotel	162.4191	162.5030	ARCSAT	237.6026	237.7632
AZT-11	101.2994	101.3999	Astrotel	163.3481	163.5552	ARCSAT	238.6125	238.7910
ARCSAT	101.8009	101.9479	Astrotel	164.3272	164.3730	ARCSAT	240.6761	240.7696
AZT-11	102.3026	102.3989	Astrotel	165.3199	165.3783	ARCSAT	241.6335	241.6479
AZT-11	103.3278	103.3990	Astrotel	166.3182	166.5588	ARCSAT	243.5402	243.7413
ARCSAT	103.8369	103.9427	Astrotel	167.2770	167.5416	ARCSAT	245.5879	245.7663
ARCSAT	105.7937	105.9410	AZT-11	172.2505	172.3853	ARCSAT	251.5368	251.7127
ARCSAT	106.8030	106.9421	AZT-11	174.3262	174.4515			
ARCSAT	107.8002	107.9490	AZT-11	177.2540	177.3501			

the MaxIM DL program. The photometric comparison star had coordinates $20^h23^m35^s.358$, $+64°36'56''.66$ from the USNO-A2.0 catalog [39]. Magnitudes of $V = 16^m.33$, $R = 15^m.58$ were obtained for it [33].

TABLE 1b. Observation Log

Telescope	Start-end of observations JD-2456000		Telescope	Start-end of observations JD-2456000		Telescope	Start-end of observations JD-2456000	
2017								
AZT-11	872.3866	872.5187	AZT-11	917.3226	917.5159	KFU	937.3274	937.5038
AZT-11	873.3987	873.5308	AZT-11	918.3310	918.3918	18cm SL	937.4928	937.5441
AZT-11	874.3920	874.5283	AZT-11	920.2974	920.4001	KFU	938.3639	938.5113
AZT-11	875.4606	875.5437	AZT-11	921.3837	921.5033	18cm SL	938.4675	938.4675
AZT-11	876.4163	876.5442	Zeiss 60	923.4867	923.5589	Zeiss 60	940.2881	940.2966
AZT-11	890.2972	890.5071	18cm SL	924.3025	924.4847	AZT-11	945.3496	945.3581
ZTSh	891.2792	891.5451	AZT-11	925.3143	925.5136	AZT-11	946.3060	946.3124
ZTSh	892.2714	892.5391	K-380	926.3344	926.5006	AZT-11	948.2775	948.2860
AZT-11	893.3906	893.5314	18cm SL	926.4129	926.5532	Zeiss 60	969.5778	969.5787
AZT-11	897.3600	897.3702	Zeiss 60	927.4650	927.4849	Zeiss 60	982.5705	982.5956
AZT-11	898.2945	898.5338	Ê-380	928.3890	928.3890	Zeiss 60	983.5471	983.5879
AZT-11	899.3637	899.4376	Zeiss 60	928.4927	928.5466	Zeiss 60	984.5018	984.5833
AZT-11	900.3718	900.5125	Zeiss 60	929.4570	929.5459	Zeiss 60	1022.5852	1022.5870
AZT-11	901.3487	901.5141	K-380	930.4051	930.5297	AZT-5	1070.3568	1070.4636
AZT-11	902.3702	902.5075	K-380	931.3287	931.3820	AZT-5	1071.3661	1071.3661
AZT-11	903.2869	903.4734	AZT-11	933.3498	933.3964	AZT-5	1072.1438	1072.1835
AZT-11	904.3219	904.4486	18cm SL	933.5089	933.5544	AZT-5	1075.2020	1075.2429
AZT-11	905.3391	905.5325	AZT-11	934.2986	934.3177	Zeiss 60	1080.3402	1080.4903
AZT-11	906.2832	906.5342	Zeiss 60	934.4922	934.5597	Zeiss 60	1081.1864	1081.2381
AZT-11	908.4299	908.5108	AZT-11	935.3111	935.5047	Zeiss 60	1082.1528	1082.4748
AZT-11	912.3773	912.4864	AZT-11	936.3388	936.3769	Zeiss 60	1083.2772	1083.4195
AZT-8	915.3621	915.4892	18cm SL	936.4961	936.5517	ZTE	1085.1400	1085.2306
AZT-11	916.3022	916.3972	AZT-11	937.3211	937.3719	AZT-8	1101.3035	1101.3985

3. Outburst light curves for 2012 and 2017

The observations in 2012 cover the interval from JD = 2456082 through JD = 2456251 and contain 82 observation nights. Over this time we recorded 4 normal outbursts, one superoutburst, and one fragment presumably belonging to a second superoutburst. In 2013, observations were made on one night. In 2017, during the interval from JD = 2457872 to JD = 2458083, which contains 63 observation nights, we recorded 3 normal outbursts and 2 superoutbursts (see the observation log in Tables 1a and b). The resulting outburst curves are shown in Fig. 1.

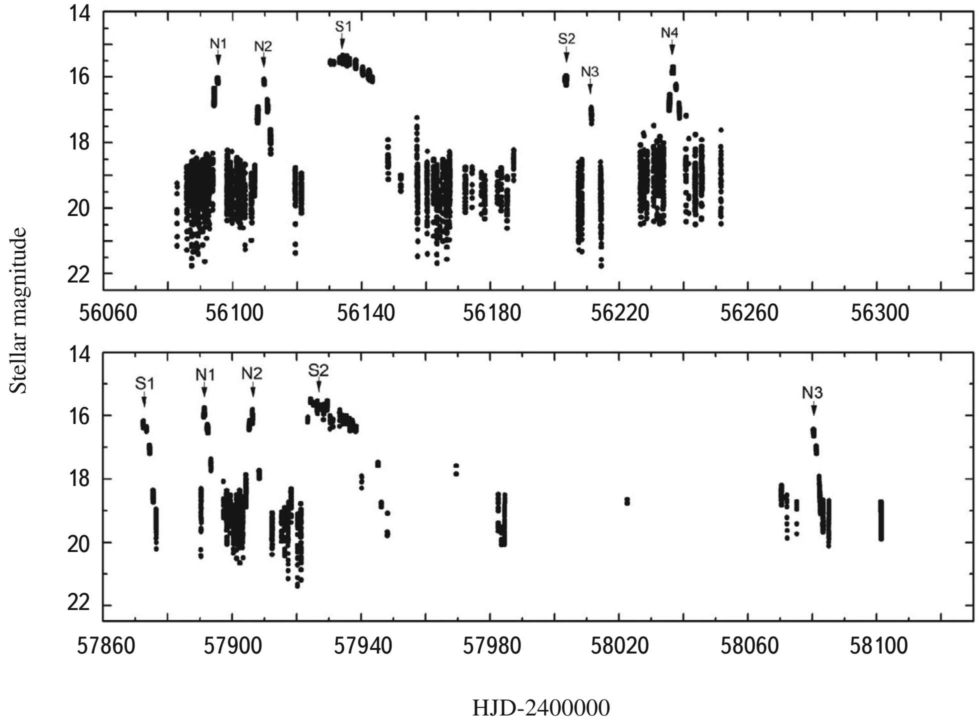

Fig. 1. Outburst light curves of the star MN Dra during 2012 (top) and 2017 (bottom). The letter N denotes normal outbursts and S, superoutbursts.

The coverage of 2012 by the observations does not allow us to reach any conclusion about the number of normal outbursts contained in a single supercycle. We can only state that there are at least two. In this same year it is also not possible to determine the duration of the system supercycle owing to an insufficient number of observations of superoutbursts S2. We can also say that in 2017, at least 2 normal outbursts were observed over a supercycle. We found the supercycle size to be ~65 days, which is greater than found in 2003, a supercycle length of ~60 days [34] but less than the value, 74±0.5 d, found in Ref. 36. In all the years of the observations, the cycle held at a level of ~15 d, as in 2009. The duration of the normal outbursts was 3-4 d, and the amplitude was 3-3.5 stellar magnitudes for both observation years. The duration S2 of a superoutburst in 2017 was 18 d, while the amplitude of the superoutbursts reached ~4^m in 2012 and in 2017.

4. Light curves

The data for all the observation nights manifest short-period oscillations in brightness, regardless of the outburst activity of the system. Some examples of individual light curves in different states of the system are shown in Fig. 2. The amplitudes of the curves vary from $0^m.06$ in normal outbursts to 2^m during the inactive state between them.

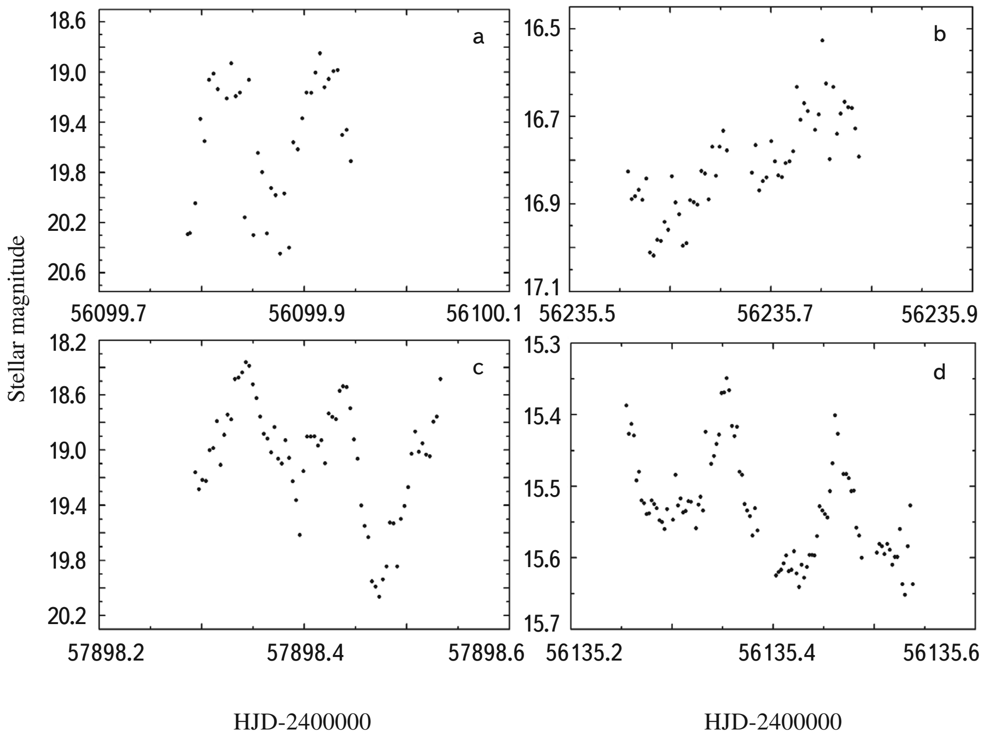

Fig. 2. Examples of individual light curves from different stages of outburst activity: (a) inactive state 2012; (b) inactive state 2017; (c) during a normal outburst, 2012; (d) during a superoutburst, 2012.

We noticed previously that the profile of the light curve of negative superoutbursts most often have an asymmetric form: the rise in brightness is slower than its fall. In this regard, the light curve obtained in 2013 is interesting (Fig. 3). It typically has a sharp rise in brightness, with a quasi-halt lasting roughly half the period and an equally rapid drop in brightness (the main hump). The sharp rises and drops in brightness took place over an average of 12 min, at a rate of 0.06-0.08 stellar magnitudes/min. In the interval between neighboring main humps, a smaller secondary hump was observed with an amplitude that rose from cycle to cycle. Data folded with the period of the negative humps show that, on the average, the presence of the secondary hump produces an asymmetric profile of the light curve. We note that Zemko, et al. [40], have also reported sporadic appearances of a secondary hump in light curves of the SU UMa-type dwarf nova ER UMa.

5. Frequency analysis of the data

For the frequency analysis we separate all the data into observations related to superoutbursts and observations related to the quiescent state and normal outbursts. These separations were applied to 2012 and 2017.

To reduce the effect on the statistical analysis of the time series owing to the dependence of the amplitude

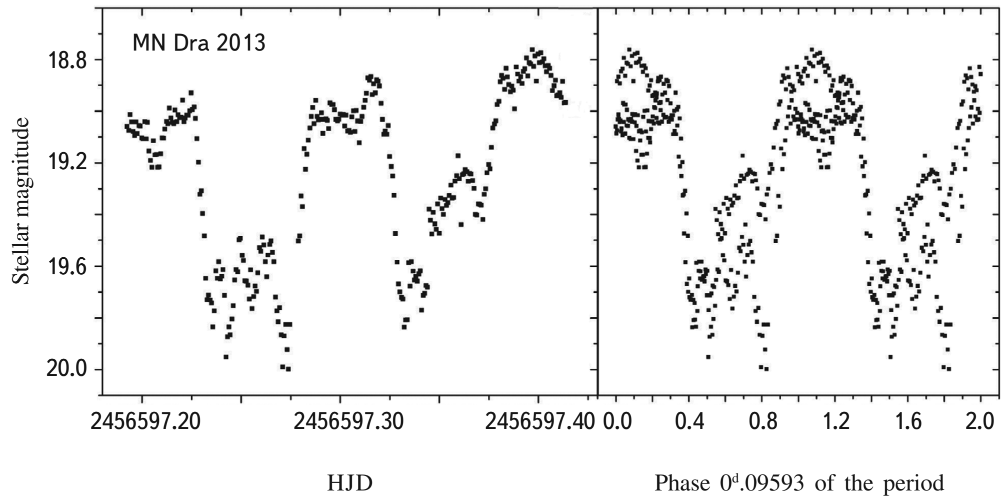

Fig. 3. An example of an unusual light curve of negative superhumps of MN Dra (left) and a phase curve for these lines (right). The curves reveal a reproducibility of the appearance of the secondary hump (but with different amplitude) from cycle to cycle during the night.

of the oscillations on the brightness of the system, the data were converted into relative intensities I according to

$$I = 10^{-0.4m} \times 10^{7} ,$$

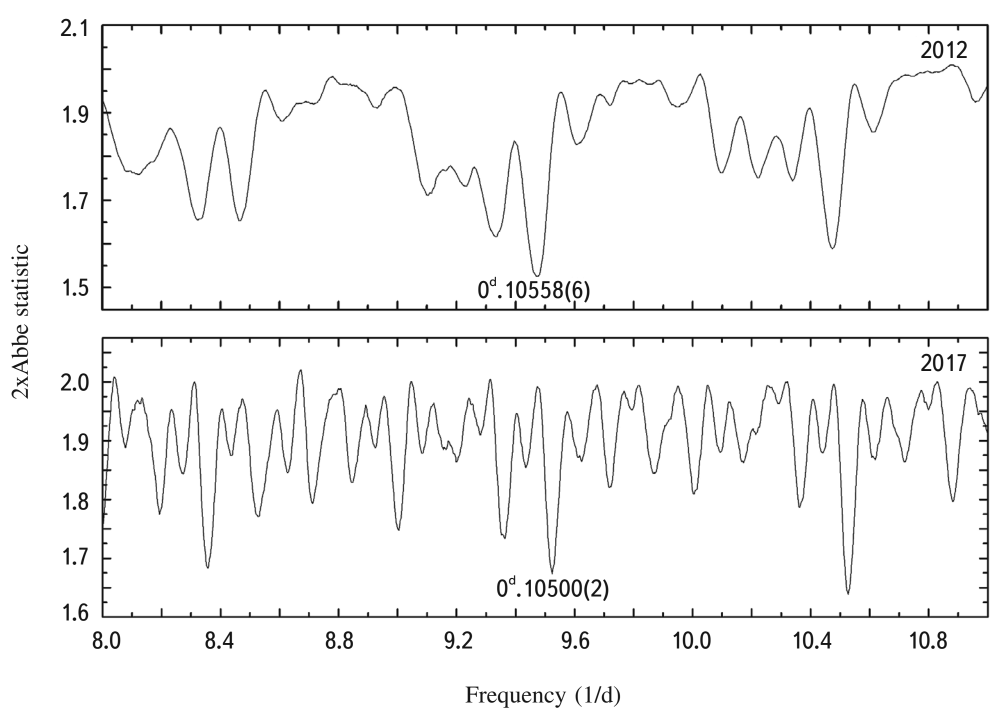

Fig. 4. Periodograms for data during superoutbursts.

where m is the stellar magnitude.

The frequency analysis employed the Stellingwerf method, which is a modification of the PDM (Phase Dispersion Minimization) method [41], in the ISDA program. The result for the superoutbursts is shown in Fig. 4.

5.1. Superoutbursts of 2012 and 2017. The strongest peak for the observations during a superoutburst of 2012 indicates a period of $0^{d}.10558(6)$ and for that of 2017, of $0^{d}.10500(2)$. We interpret them as the average periods of the positive superhumps. The difference in these values can be explained both by differing coverage of the superoutbursts in 2012 and 2017, and by possible changes in the period of the superhumps during the superoutbursts.

With the aid of a combined method for matching the well recorded profile of the superhump with the light curve studied here and a chord method, we determined the times of the maxima for all the nights where this was possible. The resulting times and amplitudes of the maxima for the superoutbursts are listed in Table 2. A detailed analysis of the changes in O-C during the superoutburst of 2012 is given by Kato, et al. [38].

Periodograms for the quiescent state and the normal outbursts are shown in Fig. 5.

TABLE 2. Times of the Superhump Maxima (HJD) and Their Amplitudes for the Superoutbursts of 2012 and 2017

HJD-2400000	Amplitude of oscillations (stellar magnitude)	HJD-2400000	Amplitude of oscillations (stellar magnitude)
2012			
56130.4398	0.0630	56135.4651	0.2015
56130.5278	0.0684	56138.2351	0.1738
56131.4242	0.0597	56140.4070	0.1695
56133.2965	0.1192	56142.5072	0.1787
56134.2773	0.1992	56143.4612	0.1074
56134.5012	0.1855	56148.3680	0.4903
56135.3535	0.1809		
2017			
57872.4497	0.121	57924.4093	0.078
57873.5015	0.101	57925.3744	0.050
57874.4470	0.121	57926.4938	0.094
57875.4997	0.234	57929.5170	0.166
57876.4561	0.565	57935.4134	0.159

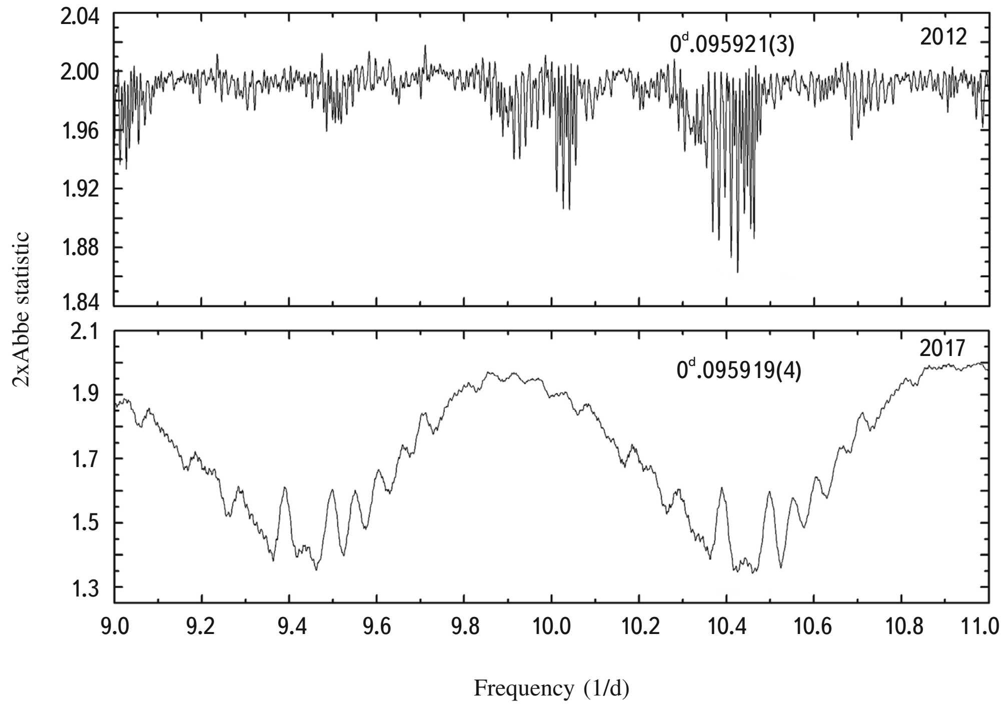

Fig. 5. Periodograms for data in the quiescent state and normal outbursts for 2012 (top) and 2017 (bottom). The frequency analysis was done for all the available data.

5.2. The inactive state and normal outbursts in 2012-2017. The strongest signal for the data of 2012 in the inactive state yields a period of $0^d.095921(3)$, which coincides with the average value of the period for the negative superhumps [35]. In the periodogram for 2017, this period also dominates (the peak is at $0^d.095919(4)$).

We note that in the periodograms for both observation seasons, the peak centered at the frequency corresponding to the period of the negative superhumps is split into finer peaks. This splitting may arise from the fact that this period undergoes changes on the scale of the observations, as noted previously [35] for this object. We analyzed the possible variations in the period using the O-C method for the maxima of the light curves.

The resulting times and amplitudes of the maxima for the quiescent state and normal outbursts are listed in Table 3.

Using the periods of the negative superhumps for each observation year and the times of the maxima of the negative superhumps, we obtain values of O-C for all the nights when this is possible. The resulting diagrams are shown in Figs. 6 (2012) and 7 (2017).

The behavior of the amplitude of the negative superhumps indicates the same dependence in all stages of outburst activity, i.e., a rise in amplitude during the quiescent state and a decrease during the times of the outbursts.

The O-C diagrams for 2012 and 2017 reveal a continuous variation in the period of the negative superhumps during the entire supercycle. This variation has a cyclical character between normal outbursts. For the cycles that are well covered by observations near the normal outbursts on JD 2456095, 2456211, 2456236, 2457891, 2457906,

TABLE 3. Times of Maxima (HJD) and Their Amplitudes for the Quiescent State and Normal Outbursts

HJD-2400000	Amplitude of oscillations (stellar magnitude)	HJD-2400000	Amplitude of oscillations (stellar magnitude)
1	2	3	4
2012			
56082.8057	1.5755	56166.4232	1.9924
56085.7851	1.603	56166.5226	2.0659
56086.7572	1.5024	56167.3866	1.4395
56087.3366	1.3617	56167.4853	1.4733
56087.8132	1.3337	56172.2681	1.1455
56088.7762	1.8237	56172.3579	1.3321
56089.3526	1.3331	56174.363	0.9531
56089.7418	1.7724	56177.3248	0.8035
56090.8022	1.1254	56178.2909	0.7344
56091.3811	1.6564	56182.3146	0.5904
56091.8646	1.602	56183.3875	0.9475
56092.4512	1.3854	56185.3043	0.9783
56092.9284	0.945	56187.3118	0.6497
56093.8955	0.9188	56207.5454	1.5859
56094.3935	0.0911	56208.3941	1.9989
56095.3345	0.0575	56211.3548	0.1811
56098.3968	1.3487	56211.4593	0.1979
56099.3538	1.0011	56214.2421	1.6874
56099.9182	1.2155	56214.3418	1.8994
56101.3552	1.1409	56214.4358	1.9076
56101.8384	1.1285	56226.6402	1.7186
56102.3178	1.37	56226.7439	1.7563
56103.3644	1.1843	56228.6464	1.4611
56103.9458	1.0341	56230.7577	1.6761
56105.8638	1.2887	56231.7222	1.5368
56106.8184	0.7398	56232.6745	1.7048
56106.9158	0.7398	56233.6411	1.7371
56107.8702	0.2943	56233.7341	1.72
56109.8816	0.0846	56235.6534	0.2014
56110.8403	0.175	56235.7546	0.177
56111.7921	0.4973	56236.6106	0.0729
56121.3466	1.0108	56236.7143	0.0757

TABLE 3. (Continued)

1	2	3	4
	2012		
56121.4377	0.9212	56237.6677	0.1045
56157.3838	1.4401	56238.7097	0.2086
56157.4779	1.4763	56240.7256	1.4948
56160.4536	1.9051	56243.5831	1.5963
56162.4716	1.2784	56243.6749	1.8094
56163.4396	1.9191	56245.6828	1.78
56163.5351	1.8327	56251.621	1.962
56165.3635	2.0625		
	2017		
57890.3925	0.965	57917.4975	2.0597
57891.3516	0.06	57918.3525	0.778
57891.4551	0.147	57920.3693	2.535
57892.3102	0.154	57921.4194	1.175
57892.4107	0.127	57982.566	0.952
57892.5025	0.146	57984.5747	1.219
57893.4533	0.091	58070.4265	0.533
57898.3416	0.737	58072.1510	1.278
57898.4306	0.869	58080.4284	0.084
57899.3948	0.679	58081.1984	0.187
57900.4483	0.923	58082.2462	0.275
57901.4065	1.109	58082.3443	0.432
57902.4643	1.033	58082.4401	0.436
57903.3388	1.154	58083.2980	0.729
57904.3866	0.636	58083.3911	0.759
57905.4516	0.1055	58085.2119	0.693
57906.5018	0.1625	58101.3190	0.813
57908.4973	0.1893	58101.4015	1.045
57916.3363	1.2478		

and, probably, an outburst that was missed during the interval JD 2456167-2456172, it can be seen that the variation in O-C changes sharply during normal outbursts. In the quiescent state between outbursts, O-C gradually increases, which corresponds to an increase in the period of the negative superhumps, while during the outburst itself the period falls off rapidly. We note that the point on the O-C diagram lying at JD=2456121 may be shifted by one period in

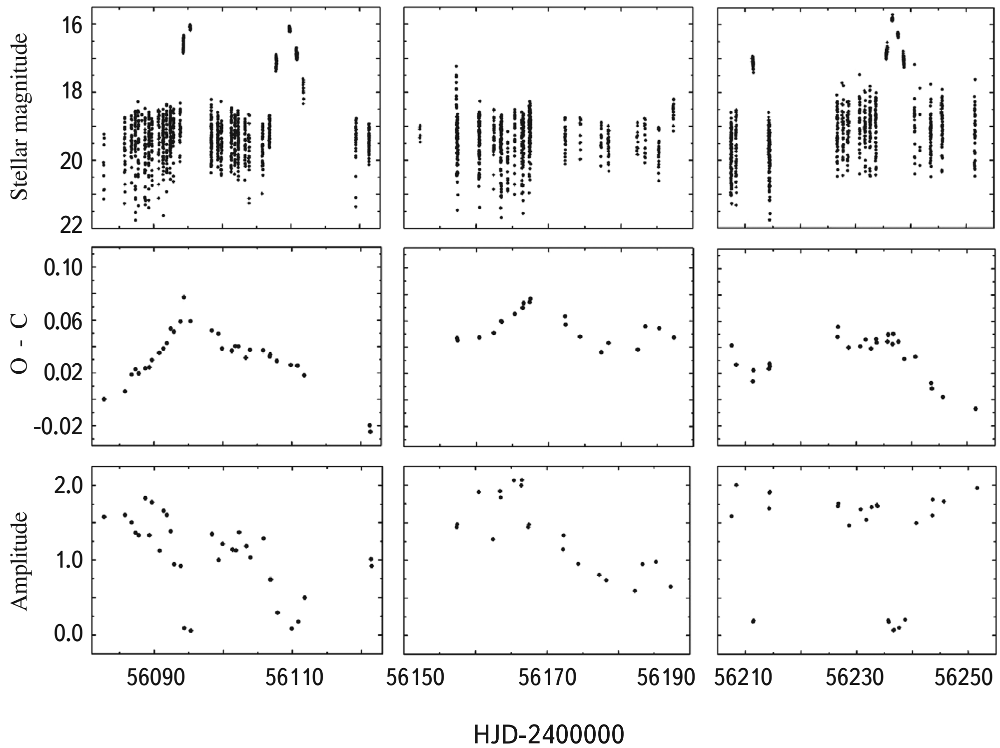

Fig. 6. From top to bottom: overall light curve; O-C diagram; a plot of the variation in the amplitude of superhumps for three sets in 2012. The large spread in the data at the minimum on individual nights is caused by a reduction in the accuracy of the observations owing to the small size of a telescope and/or weather conditions.

the upper part of the diagram, since there is a nonuniqueness owing to possible miscounting of cycles.

A similar variation in the negative superhumps was noted by Osaki and Kato [31] for the dwarf nova V1504 Cyg in data from the Kepler space telescope. In addition, O-C manifests a tendency toward a reduction in the average period of the negative superhumps during the supercycle, as demonstrated for V1504 Cyg [31] and ER UMa [42]. The results of the periodogram analysis of MN Dra are in agreement with the conclusions of the O-C analysis. As an example, Fig. 8 shows periodograms for series of observations in 2017 during one of the outbursts and in the quiescent state. According to the periodograms, the period of the negative superhumps during the outburst was $0^d.0951$, while toward the end of the quiescent state it increased to $0^d.0961$.

According to the simplified model of Larwood [15] for the retrograde precession of an inclined disk, the radius of the disk is inversely proportional to the period of the negative superhumps. In terms of this model, the pattern of the variations in O-C for MN Dra corresponds to an expansion of the accretion disk during a normal outburst and its gradual reduction during the quiescent state. Here the average radius of the accretion disk increases with rising phase of the supercycle. Variations of this kind are also predicted by the theory of thermal-tidal instability of an accretion disk [43].

6. Conclusions

Two campaigns for observations of the dwarf nova MN Dra in 2012-2017 were carried out with nine telescopes on 152 nights plus one night's observations in 2013. The observations covered four superoutbursts and seven normal outbursts, as well as the quiescent state between them.

We studied the outburst activity of the system and found that for 2017 the interval between neighboring superoutbursts was 65 days, and between neighboring normal outbursts, 15 days.

As in 2009, during 2012 and 2017 MN Dra manifested positive superhumps during superoutbursts, and negative ones during the quiescent state and in normal outbursts. The average period of the positive superhumps for 2012 turned out to be 0.10558(6) days and in 2017, 0.10500(2) days.

Periodogram analysis and an analysis of O-C of the brightness maxima of the negative superhumps revealed a cyclical variation in the period of the superhumps from one normal outburst to another. In the quiescent state, the O-C gradually increase, which corresponds to an increase in the period of the negative superhumps, while during the time of the outburst itself, the period rapidly decreases.

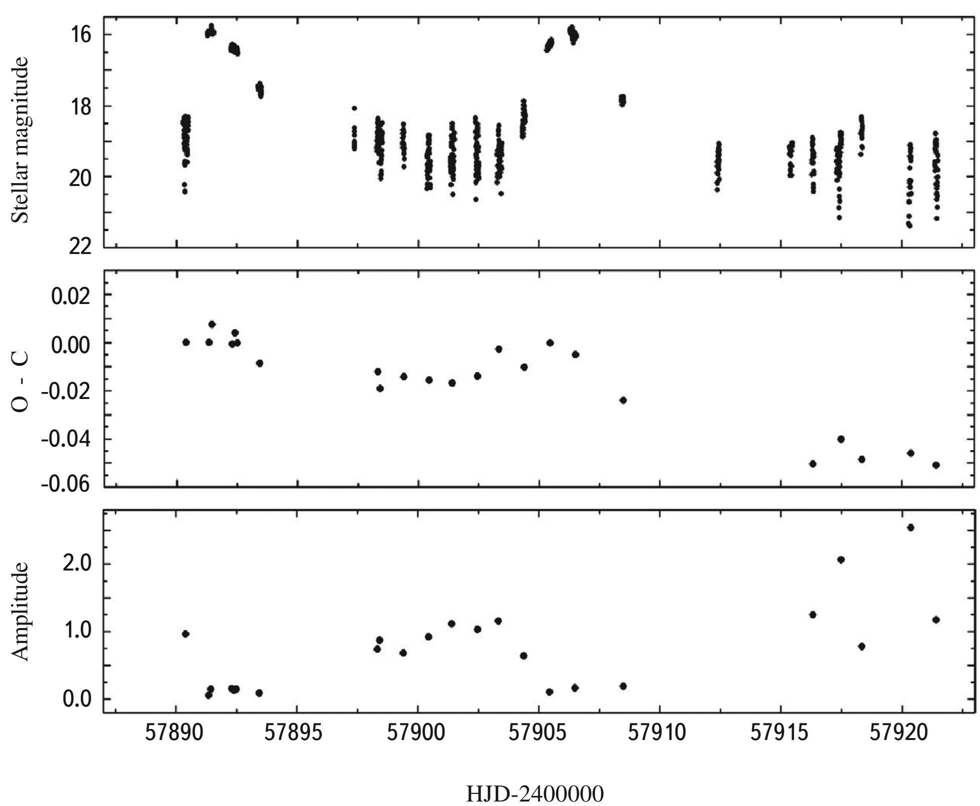

Fig. 7. From top to bottom: part of the overall light curve for 2012; O-C diagram for the maxima of the negative superhumps; a plot of the variation in their amplitude.

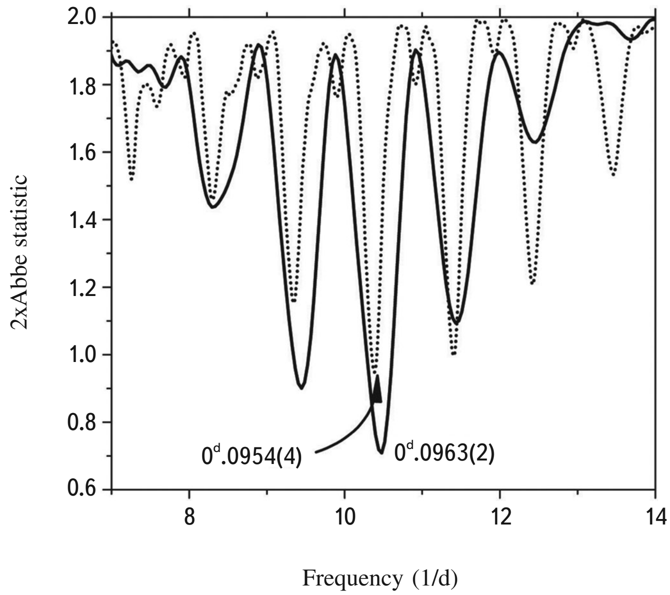

Fig. 8. Periodograms for data of 2017 in outburst N1 (two nights in the interval JD=2457891.45-2457892.46, smooth curve) and in the quiescent state (four nights in the interval JD=2457900.45-2457903.49, dotted curve),

In terms of a simplified inclined disk model [15], these kinds of changes in O-C may correspond to expansion of the accretion disk during a normal outburst and its gradual reduction in the quiescent state, which is indeed consistent with the theory of thermal-tidal instability of an accretion disk [43].

This work was partially supported by RFFI grants 18-32-00371, APVV-15-0458 and 2/008/17.

It was partially supported by a subsidy of the government of the Russian Federation intended to increase the competitiveness of Kazan Federal University among world scientific-research centers.

The work was partially carried out with subsidies provided by Kazan Federal University for carrying out a government task in the sphere of scientific activity (3.9780.2017/8.9).

Observations obtained at the Northern Caucasus Astronomical Station of KFU were used in this work.

REFERENCES

1. B. Warner, Astrophys. Space Sci. **226**, 187 (1995).
2. C. Knigge, Mon. Not. Roy. Astron. Soc. **373**, 484 (2006).
3. Y. Osaki, Publ. Astron. Soc. Pacif. **108**, 39 (1996).
4. T. Kato, A. Imada, M. Uemura, et al., Publ. Astron. Soc. Japan **61**, S395 (2009).

5. D. Harvey, et al., Publ. Astron. Soc. Pacif. **107**, 551 (1995).
6. J. Patterson, et al., Publ. Astron. Soc. Pacif. **109**, 468 (1997).
7. M. A. Wood and C. J. Burke, Astrophys. J. **661**, 1042 (2007).
8. P. Barrett, D. O'Donoghue, and B. Warner, Mon. Not. Roy. Astron. Soc. **233**, 759 (1988).
9. P. Barrett, D. O'Donoghue, and B. Warner, Mon. Not. Roy. Astron. Soc. **236**, 735 (1989).
10. S. B. Foulkes, C. A. Haswell, and J. R. Murray, Mon. Not. Roy. Astron. Soc. **366**, 1399 (2006).
11. J. Smak, Acta Astronomica **59**, 419 (2009).
12. M. M. Montgomery, Astrophys. J. Lett. **745**, L25 (2012).
13. M. M. Montgomery, Astrophys. J. Lett. **753**, L27 (2012).
14. J. D. Larwood, R. P. Nelson, J. C. B. Papaloizou, et al., Mon. Not. Roy. Astron. Soc. **282**, 597 (1996).
15. J. Larwood, Mon. Not. Roy. Astron. Soc. **299**, L32 (1998).
16. S. H. Lubow, Astrophys. J. **398**, 525 (1992).
17. J. R. Murray and P. J. Armitage, Mon. Not. Roy. Astron. Soc. **300**, 561 (1998).
18. S. Horn and W. Kundt, Astrophys. Space Sci. **158**, 205 (1989).
19. P. R. Maloney, M. C. Begelman, and J. E. Pringle, Astrophys. J. **472**, 582 (1996).
20. P. R. Maloney and M. C. Begelman, Astrophys. J. **491**, L43 (1997).
21. P. R. Maloney, M. C. Begelman, and M. A. Nowak, Astrophys. J. **504**, 77 (1998).
22. G. I. Ogilvie and G. Dubus, Mon. Not. Roy. Astron. Soc. **320**, 485 (2001).
23. J. E. Pringle, Mon. Not. Roy. Astron. Soc. **281**, 357 (1996).
24. R. A. M. J. Wijers, and J. E. Pringle, Mon. Not. Roy. Astron. Soc. **308**, 207 (1999).
25. J. R. Murray, D. Chakrabarty, G. A. Wynn, et al., Mon. Not. Roy. Astron. Soc. **335**, 247 (2002).
26. D. Lai, Astrophys. J. **524**, 1030 (1999).
27. H. P. Pfeiffer and D. Lai, Astrophys. J. **604**, 766 (2004).
28. M. M. Montgomery, Mon. Not. Roy. Astron. Soc. **394**, 1897 (2009).
29. T. Ohshima, et al., Publ. Astron. Soc. Japan **64**, L3 (2012).
30. T. Ohshima, et al., Publ. Astron. Soc. Japan **66**, 67 (2014).
31. Y. Osaki, and T. Kato, Publ. Astron. Soc. Japan **65**, 95 (2013).
32. M. Still, et al., Astrophys. J. Lett. **717**, L113 (2010).
33. S. V. Antipin and E. P. Pavlenko, Astron. Astrophys. **391**, 565 (2002).
34. D. Nogami, M. Uemura, R. Ishioka, et al., Astron. Astrophys. **404**, 1067 (2003).
35. E. P. Pavlenko, et al., Astron. Rep. **54**, 6 (2010).
36. K. Bakowska, et al., Astron. Astrophys. **603**, 72 (2017).
37. E. P. Pavlenko, et al., AIP Conference Proceedings, **1273**, 320 (2010).
38. T. Kato, et al., Publ. Astron. Soc. Japan **66**, 90 (2014).
39. D. Monet, et al., USNO-A2.0, A Catalog of Astrometric Standards (U. S. Naval Observatory, Washington, DC) (1998).

40. P. Zemko, T. Kato, and S. Shugarov, Publ. Astron. Soc. Japan **65**, 54 (2013).

41. R. F. Stellingwerf, Astrophys. J. **224**, 953 (1978).

42. P. Zemko, S. Shugarov, T. Kato, et al., Contributions of the Astronomical Observatory Skalnaté Pleso **43**, 319 (2014).

43. Y. Osaki, Publ. Astron. Soc. Japan **41**, 1005 (1989).